



---

## Antibacterial Activity of Silver-Modified Bacterial Cellulose Produced from Coconut Water for Wound Dressing Application

Anastasia Wheni Indrianingsih\*, Roni Maryana, Vita Taufika Rosyida, Wuri Apriyana, Tri Hadi Jatmiko and Septi Nur Hayati

Research Unit for Natural Product Technology, Indonesian Institute of Sciences, Gading, Playen, Gunungkidul, Yogyakarta, 55581, Indonesia

**Abstract** This study aims to synthesize silver-modified bacterial cellulose from local waste coconut water and evaluate its antibacterial activity for wound dressing application. Silver-modified bacterial cellulose (Ag-BC) was synthesized by immersing the bacterial cellulose in silver nitrate solution. Sodium borohydride ( $\text{NaBH}_4$ ) was used to reduce the absorbed silver ion ( $\text{Ag}^+$ ) to the metallic silver nanoparticles ( $\text{Ag}^0$ ) inside of bacterial cellulose. AgNPs (Ag Nanoparticles) were chemically bonded to the bacterial cellulose surface. Ag-BC composite were characterized using Scanning Electron Microscopy (SEM), X-ray diffraction (XRD), Energy Dispersive X-ray spectroscopy (EDX) and Fourier Transform Infrared spectroscopy (FTIR). Antibacterial activity of Ag-BC composites were performed against the *Escherichia coli* (Gram-negative), *Staphylococcus aureus* (Gram-positive), *Pseudomonas aeruginosa* and *Salmonella typhi* by comparing with antibiotic standard streptomycin by disk diffusion methods. The neat fibril network of Ag-BC composites was observed using a Scanning Electron Microscopy (SEM) analysis. A highly crystalline of Ag-BC film was observed in X-ray diffraction (XRD) measurements and the presence of metallic silver was confirmed using EDX. The room temperature-dried Ag-BC composite also exhibited high antimicrobial activity against *Escherichia coli* (Gram-negative), *Staphylococcus aureus* (Gram-positive), *Pseudomonas aeruginosa* and *Salmonella typhi*. The results obtained for the antibacterial activities in Ag-BC composites confirmed the potential of this material in a wound dressing application.

**Keywords** coconut water, bacterial cellulose, silver nanoparticles, antibacterial activity

---

### Introduction

Cellulose is an insoluble water compound normally found in plant cell walls, that plays an important role in the integrity of plant cell walls [1]. Cellulose fibers from plants are known as microfibrils that are 2-20 nm in diameter and form a strong network within the cell wall of the plant. Cellulose molecules can be arranged up to thousands of microfibrils chain units of D-glucose linked by hydrogen bonding [2]. Cellulose can be produced by a fermentation process. Bacteria that can be used to produce cellulose are Acetobacter strains, Gluconacetobacter, Agrobacter, Sarcina, among others which includes non-pathogenic bacteria and is known as cellulose bacteria [3, 4]. *Acetobacter xylinum* has been known to produce pure cellulose for more than 100 years. Bacterial cellulose produced by bacterium *Acetobacter xylinum* can produce high aspect ratio nanofibers with three-dimensional porous networks [5, 6]. *A. xylinum* has been isolated from rotting sugary fruits, vegetables and fermenting coconut water [7]. Actually cellulose from plants and bacteria has the same chemical structure, but the cellulose produced by the bacteria has better fiber composition. Bacterial cellulose is a polysaccharide consisting of several hundred to thousands units of



D-glucose associated with  $\beta$  bond (1 $\rightarrow$ 4). The fibers of the bacterial cellulose usually have a diameter of more than 50 nm. The cellulose fiber units are interconnected to form a network structure, consisting of a three dimensional network of microfibrils and nanofibrils [8, 9]. Bacterial cellulose is pure and exhibits a higher degree of crystallinity than the cellulose obtained from plant in which the cellulose fibrils are embedded with lignin and hemicelluloses [3]. As already known, the lignin and hemicellulose that make up the cell wall components of plants is difficult to remove in the purification process. Thus, bacterial cellulose could be processes further without hazardous by-products and using low energy on the purification process.

Bacterial celluloses have transparent properties found by Klemm et al 2001 [10]. These properties can be identified during the purification and drying process of cellulose microbial on the surface of culture. After the filtering and drying process, a thin layer of bacterial cellulose can be observed transparently by placing colored paper. Bacterial cellulose has a greater water absorption capacity than plant cellulose. This is because the hydrogen bond in the bacterial cellulose is stronger and the bacterial cellulose polymer chain is also longer [11]. Applications of bacterial cellulose are extensive in many industries, such as in biomedical industries, paper production, food industries, and cosmetics. In the field of biomedical industries, bacterial cellulose can be used as biosensor, biofill, transdermal drug delivery, and wound cover [11-13]. In paper making, bacterial cellulose is used in the production of synthetic paper, insulation materials, and surface coatings. In the process of food manufacturing, bacterial cellulose is used as a stabilizer agent, making Nata de Coco, and baking [14], whereas in the cosmetic field, bacterial cellulose has been used as a health tonic drink and artificial nails [15]. Another advantage of BC is the presence of surface hydroxyl groups that makes it suitable for modification with various nanomaterials. BC is considered as a natural wound dressing material because of its high porosity with nanofibrous network and higher water-retention capability [16]. However, pure BC does not show any antimicrobial activity; therefore it is needed to modify BC with some antimicrobial agent to make it applicable in wound dressing and to avoid secondary infection.

Silver and its compound, either as nanoparticles, oxides or ionic forms have been known to have excellent antimicrobial activities [16-18]. Silver ions interact against bacteria in several ways; for example interact with thiol groups of enzyme and proteins that are important for bacterial respiration [19] and also can interact with the bacterial cell wall, altering the function of the bacterial cell membrane [20]. One of the advantageous properties of silver compare to other microbial agents is its higher toxicity microorganism while exhibiting lower toxicity to mammalian cells [21]. Thus, silver and its compounds were the potential candidates for preventing the infection of the wounds. However, in the case of typical application like wound dressing treatment, silver has to be retained inside a solid support to properly apply over the affected area. For this reason, BC is the potential candidate as the solid support for silver modification materials because of its high porosity and water permeability. In this study, the synthesis of bacterial cellulose by utilizing local waste of coconut water had been conducted. The resulted BC was then modified with silver to make BC-Ag composite and evaluated for its antibacterial activities. This study may be used as preliminary study in the evaluation of silver modified bacterial cellulose film as a promising candidate for application in biomedical industries especially in wound dressing applications.

## Experimental

### Reagents and General Instrumentation

*Acetobacter xylinum* (strain FNC-0001), *Pseudomonas aeruginosa*, *Eschericia coli*, *Salmonella typhi* and *Staphylococcus aureus* were purchased from Gadjah Mada University (UGM). Coconut water was obtained from Yogyakarta Province, Indonesia. Streptomycin was purchased form Oxoid. Yeast extract, sucrose , acetic acid, distilled water, urea, NaOH, silver nitrate ( $\text{AgNO}_3$ ), sodium borohydride ( $\text{NaBH}_4$ ), universal pH paper, plate count agar were purchased from Merck. The equipments used in this study were glassware, scales, autoclave, oven, desiccator, hot plate, a pH meter, Universal Testing Instrument (Lloyd UTM Zwick ZO.5), calipers, Scanning Electron Microscopy (SU-3500, Hitachi, Tokyo, Japan), Fourier Transform Infrared spectroscopy (8201 PC Shimadzu, Japan), X-ray diffractometer (Rigaku Smartlab, Japan), Field Emission Scanning Electron Microscopy (FE-SEM JEOL, Japan), and Energy Dispersive X-ray spectroscopy (JEOL, Japan).



### Media Culture and Bacterial Cellulose Production

The procedure used is a modification of Almeida et al, 2014 [22] with several modifications. The culture medium used for the fermentation of *A. xylinum* to produce bacterial cellulose consist of coconut water (1 litre), sucrose (50 g), urea (10 g), starter of *A. xylinum* (10%) and the pH is set to be pH 5 with acetic acid. The media was then sterilized by autoclave at 121°C for 15 minutes. Bacterial cellulose was grown at room temperature and static conditions for 7 days in a Petri dish. After incubation, the resulting bacterial cellulose was harvested and purified by boiling in distilled water for 2 hours, and rinsed in running water until neutral. The drying of bacterial cellulose was conducted at room temperature for 24 hours.

### Preparation of Ag-BC Nanocomposites

The preparation of Ag-BC nanocomposites was conducted according to Maneerung et al, 2008 [17] with several modifications. BC pellicles were impregnated with silver by immersing the BC in 0.001 M AgNO<sub>3</sub> for 1 h, followed by rinsing with ethanol, and then silver ion in BC were reduced in NaBH<sub>4</sub> with ratio of NaBH<sub>4</sub>:AgNO<sub>3</sub> of 100:1; 50:1 and 10:1. The excess chemicals were rinsed with large amount of distilled water. The obtained samples were dried at room temperature for 24 h for further characterization.

### Characterization

Morphological characterizations of the Ag-BC samples were performed on SEM (SU-3500 Hitachi) and FE-SEM (JEOL), operating at 15 kV at a magnification of 10,000. The formation of silver nanoparticles was identified by the XRD (Rigaku Smartlab) using Cu-K $\alpha$  radiation ( $\lambda=1.5418 \text{ \AA}$ ), operating at 40 kV and 30 mA with a step size of 0.01° and 5 s dwell time. FTIR spectra were recorded on 8201 PC Shimadzu, Japan at a frequency range of 4000-400 cm<sup>-1</sup> with the resolution of 4 cm<sup>-1</sup> and 32 scans for each sample. Elemental analysis was performed on EDX (JEOL).

### Swelling Measurement

The swelling percentage was determined using method by Maneerung et al, 2008 [17] with little modifications. Ag-BC nanocomposite were cut into a size of 2 cm width x 2 cm length and immersed in the distilled water for 72 hours. Swelling capacity was calculated as follows:

$$\text{Swelling} = (G_{s,t} - G_i) / G_i$$

where  $G_i$  is the initial weight of dried sample and  $G_{s,t}$  is the weight of sample in swollen state.

### Antibacterial Activity Evaluation

The antibacterial activity of Ag-BC pellicles was evaluated by the disk diffusion methods against *P. aeruginosa*, *E. coli*, *S. typhi* and *S. aureus*. The disk diffusion method was performed on an LB nutrient medium solid agar petri dish. The silver nanoparticle-impregnated BC was cut into a disk shape of 10 mm diameter and sterilized at 120 °C for 15 minutes. Then, the disks were placed on the agar plate inoculated with  $1 \times 10^9$  cfu/mL of bacteria and at 37 °C for 24 h. Pure BC pellicles and standard streptomycin were also incubated under the same conditions as control. The antibacterial activities of the samples were monitored by observing the inhibition zone formed surrounding the pellicles. The inhibition zone length was counted by averaging three independent experiments.

## Results and Discussion

### Morphology structure of Ag-BC composites

The morphology of the surface structure of the pure BC and Ag-BC composites was analyzed using SEM (SU-3500 from Hitachi, Tokyo, Japan) with 10,000 magnifications. Figure 1 shows the SEM image of the surface of the pure BC and Ag-BC composites.



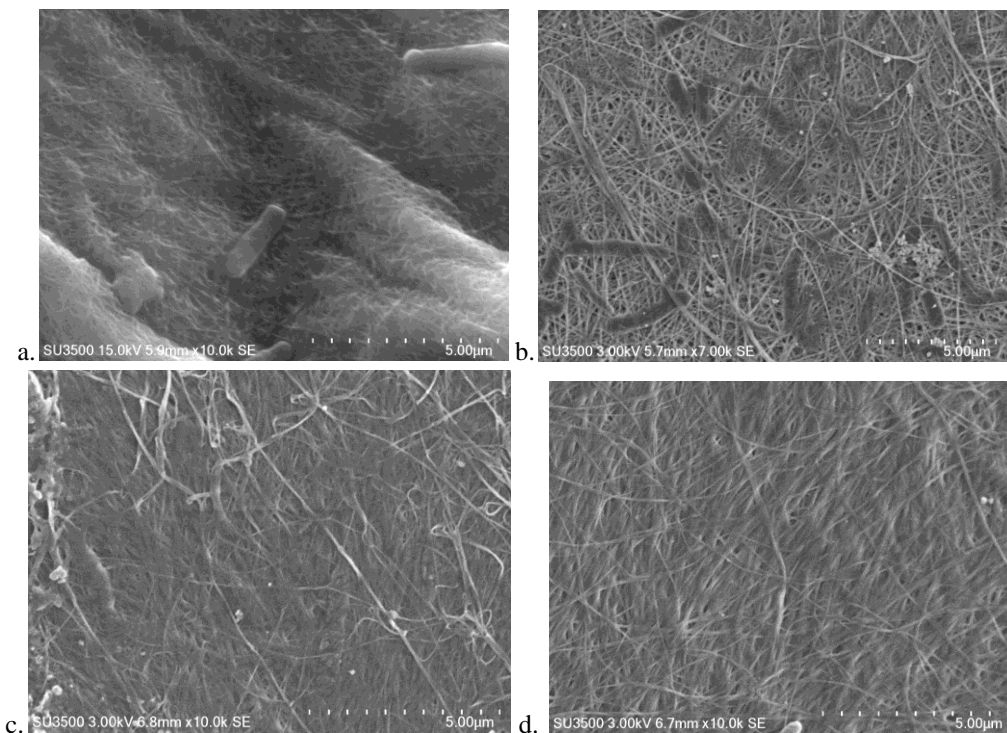


Figure 1: SEM image of room temperature-dried (a) pure BC; and Ag-BC nanocomposites that was prepared from  $\text{NaBH}_4:\text{AgNO}_3$  molar ration of (b) 10:1 (c) 50:1 and (d) 100:1.

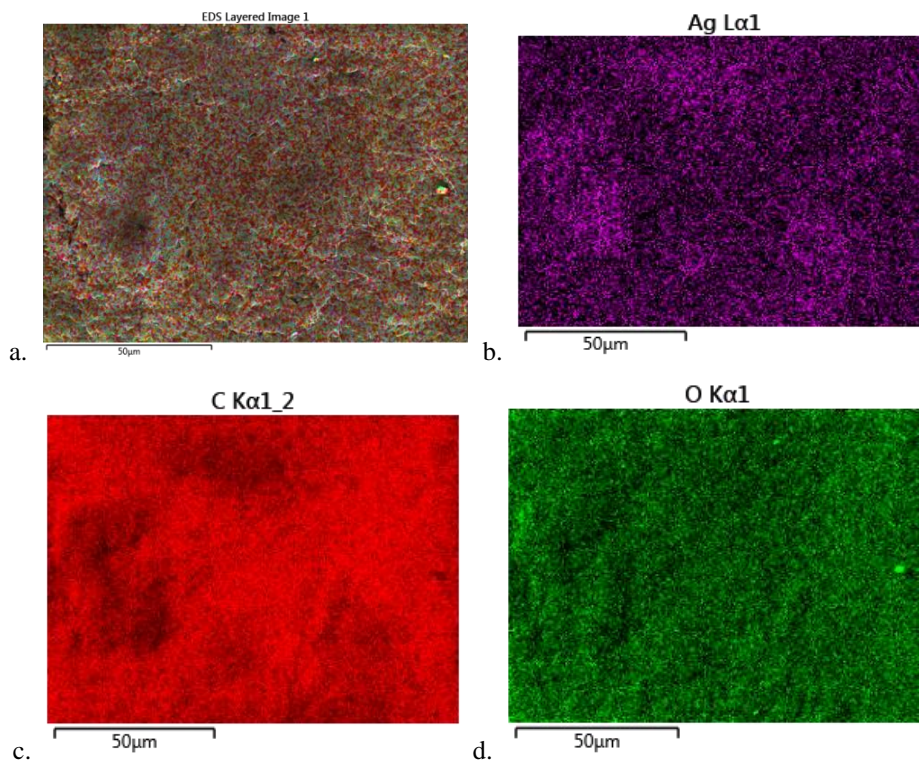


Figure 2: Energy dispersive X-ray spectrometric (EDX) elemental mapping performed on Ag-BC composite showing the combined distribution of (a) Carbon (K-series), Oxygen (K-series) and Silver (L-series), and individual distribution of (b) Ag, (c) C, and (d) O.

Pure BC is composed of mainly 50-60 nm diameter cellulose nanofibers, forming a 3D network porous structure. The nanometer-sized fibers are distributed and interconnected in such a way so as to form a finely woven porous structure. This special characteristic helps the silver ions to diffuse into the spongy structure and distribute evenly through the material as well as along the cellulose nanofiber surfaces. Structure of BC is 3D networks and consists of many pores, so that silver ion from  $\text{AgNO}_3$  was penetrated into BC through their pores. The  $\text{Ag}^+$  were bound to BC probably via electrostatic interactions because of the oxygen atoms of BC (electron-rich) are expected to interact with metal cations (electropositive) [26].

The EDX elemental mapping (Figure 2) shows quite a homogeneous distribution of silver along the fibers on BC surfaces.

In this study, three formula of  $\text{NaBH}_4:\text{AgNO}_3$  molar ratio was used (10:1, 50:1 and 100:1). The composition of elements in the Ag-BC composites was presented in Table 1.

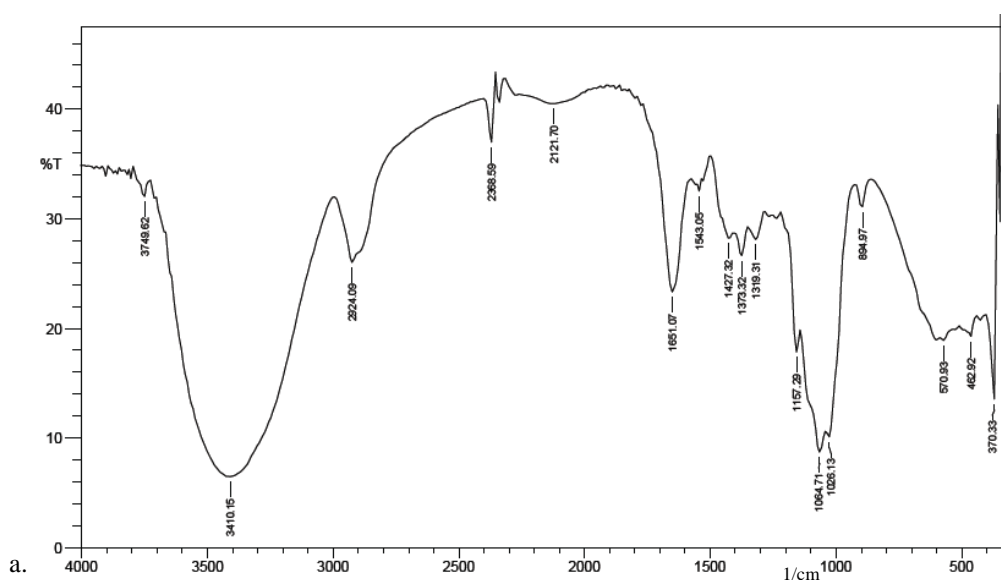
**Table 1:** The composition of element in the Ag-BC nanocomposite

$\text{NaBH}_4:\text{AgNO}_3$ molar ratio	% Element					
	C	O	Ag	Na	B	Total
10:1	43.02	56.73	0.25	-	-	100
50:1	40.25	55.72	0.30	3.73	1	100
100:1	51.52	46.50	1.98	-	-	100

The composition of Ag in the composites was increased by increasing the  $\text{NaBH}_4:\text{AgNO}_3$  molar ratio. However, boron (B) that can cause tissue damage was not found in the composites. The  $\text{NaBH}_4:\text{AgNO}_3$  molar ratio influenced the depth of silver NPS inside BC. At the higher  $\text{NaBH}_4:\text{AgNO}_3$  molar ratio, silver NPS which formed inside BC to form Ag-BC nanocomposite were deeper, this happened because the concentration of absorbed  $\text{Ag}^+$  inside BC is lower than the concentration of  $\text{Na}^+$  of the aqueous  $\text{NaBH}_4$ . It will cause the cation gradient occurred in which  $\text{Na}^+$  in the aqueous  $\text{NaBH}_4$  penetrate into BC while  $\text{Ag}^+$  not penetrate out [17].

### FTIR and XRD Characterizations

FTIR spectroscopy is often used as a method for determining specific functional groups or chemical bonds contained in a material. Figure 3 shows the FTIR spectra of BC and Ag-BC composite.



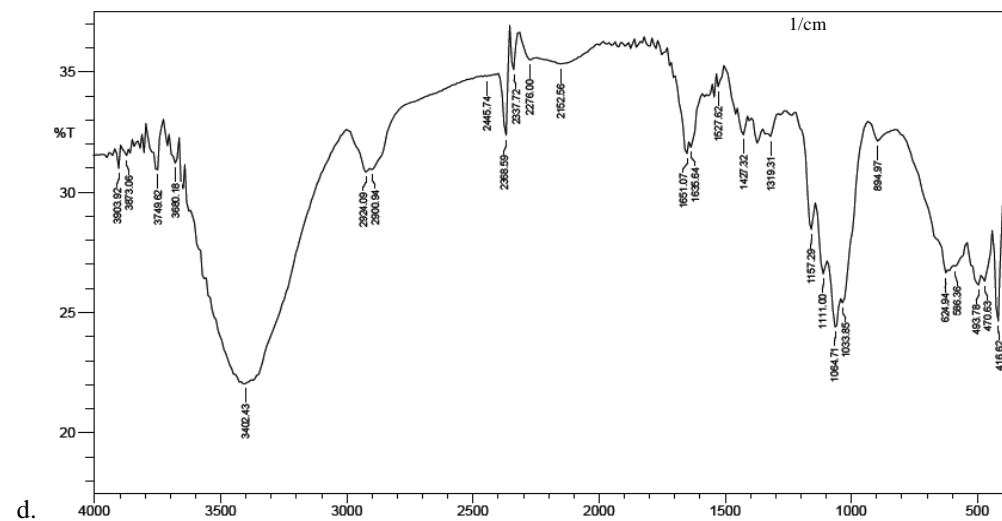
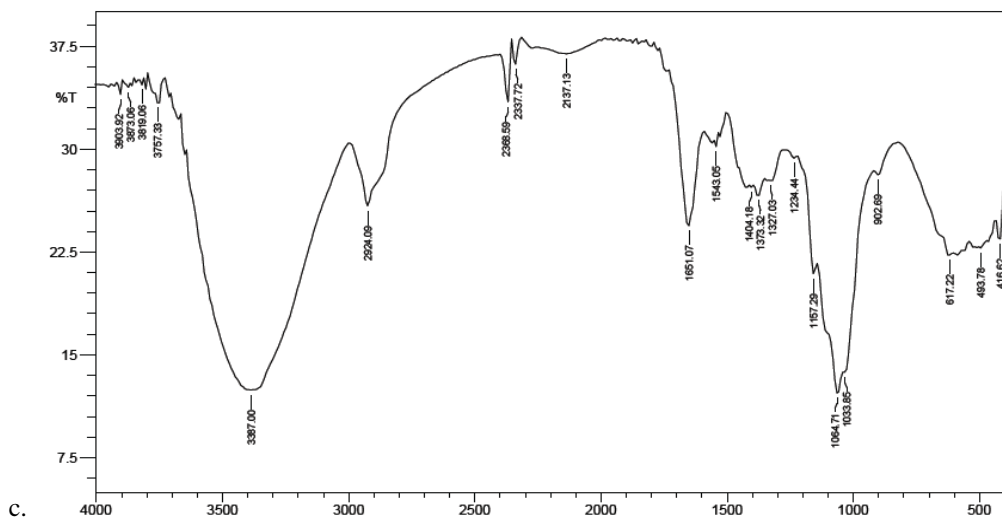
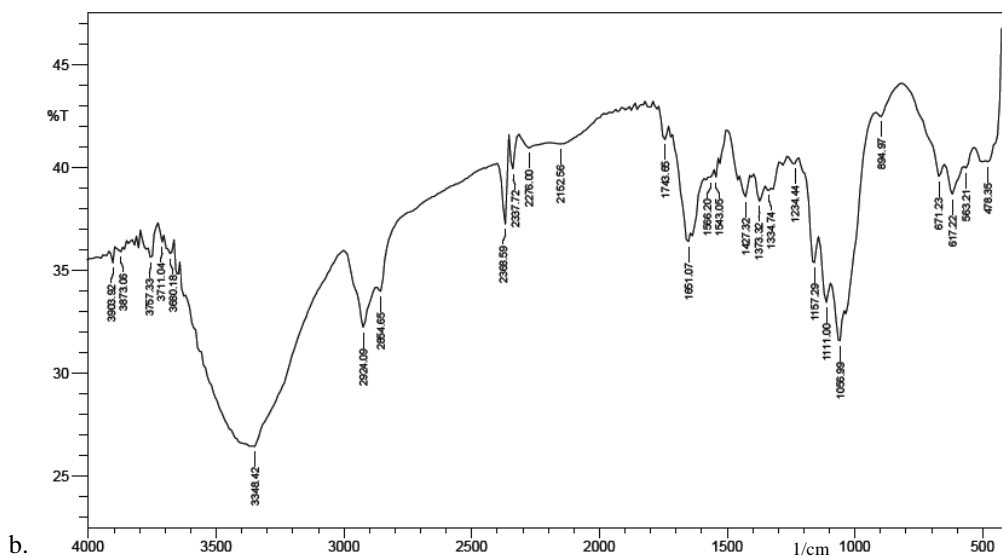


Figure 3: FTIR spectra of pure BC (a) and composite Ag-BC with molar ratio of  $\text{NaBH}_4$ :  $\text{AgNO}_3$  of 10:1 (b), 50:1 (c) and 100:1 (d).

The FTIR spectra of pure BC and Ag-BC composites were performed between  $4000\text{-}500\text{ cm}^{-1}$ . The broad vibration band around  $3300\text{-}3500\text{ cm}^{-1}$  region is assigned to the OH stretching vibration of the hydroxyl groups present in the BC network [21]. A band at  $1425\text{ cm}^{-1}$  and two smaller bands at  $2800\text{-}2930\text{ cm}^{-1}$  are assigned to the stretching vibrations of CH and  $\text{CH}_2$ , respectively [25]. The absorption peak at  $1157\text{ cm}^{-1}$  is coming from the C-O-C stretching vibration of the pure cellulose matrix, while a group of absorption at region  $1200\text{-}950\text{ cm}^{-1}$  arises due to the C-O and C-C stretching vibrations of the cellulose network.

The XRD analysis was used to examine the crystallinity of pure BC and Ag-BC composites. Figure 4 show the XRD pattern of pure BC and Ag-BC composites.

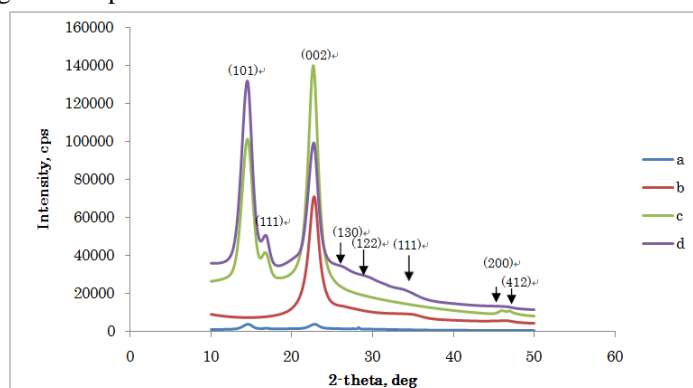


Figure 4: XRD pattern of pure BC (a) and Ag-BC composites with  $\text{NaBH}_4$ : $\text{AgNO}_3$  molar ration of 10:1 (b), 50:1 (c) and 100:1 (d).

The appearance of strong diffraction peaks at  $2\Theta$  of  $14.5$ ,  $16.8$ ,  $22.6$ ,  $27.8$ ,  $29.4$  and  $46.5^\circ$  are possibly attributed to the Miller indices of the diffraction planes of (101), (111), (002), (130), (122) and (412), respectively of crystalline cellulose [23]. These diffraction planes correspond to the highly crystalline native cellulose and it is noteworthy that the Ag-BC composites retains a similar crystallinity. The Ag-BC composites shows high cristallinity and some additional diffraction peaks at  $38.1^\circ$  and  $44.2^\circ$  are reflections of (111) and (200) of face-centered cubic metallic silver [16].

### Swelling Ability

The percentage of swelling capability was determined by the method performed by Maneerung *et al*, 2008 [17] with slight modification. Figure 5 shows high swelling ability of room temperature-dried Ag-BC composites after immersing in the distilled water for 72 h.

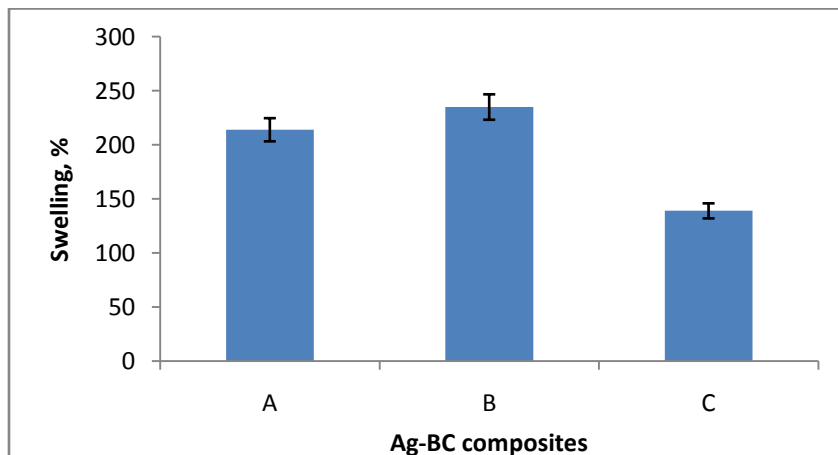
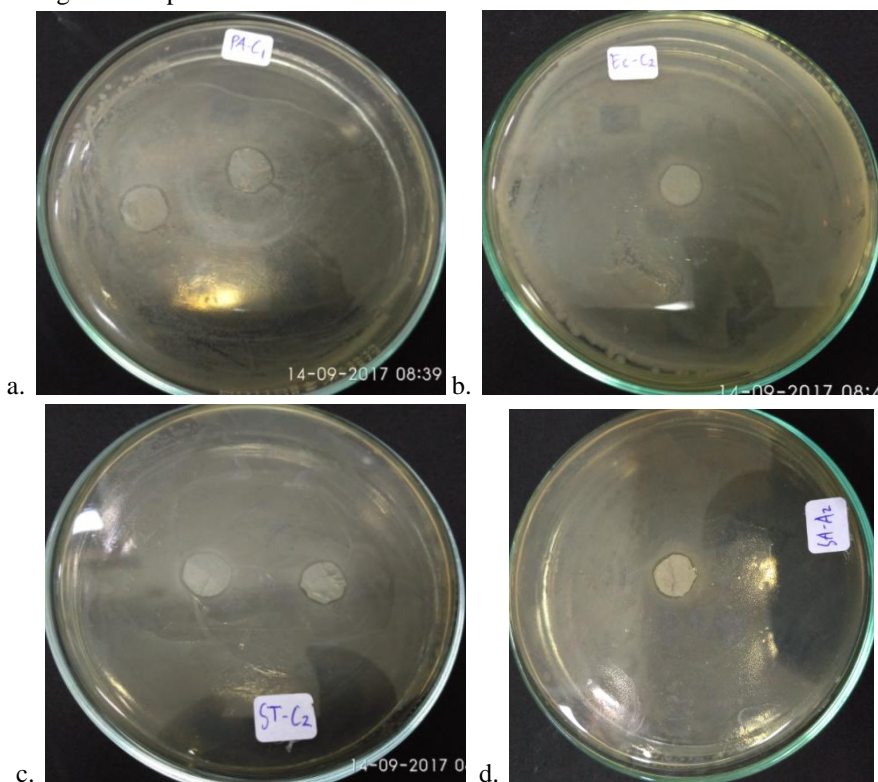


Figure 5: Swelling ability of Ag-BC composites with  $\text{NaBH}_4:\text{AgNO}_3$  molar ration of 10:1 (A), 50:1 (B) and 100:1 (C).

It is seen that from Figure 5, the highest percentage of swelling is owned by a thin layer of Ag-BC composite with a molar ratio of reducing  $\text{NaBH}_4:\text{AgNO}_3$  (50: 1) of 235.6% followed by Ag-BC (10: 1) and (100: 1) with 214,7% and 139,6% , respectively. This high swelling ability is probably due to both chemical and physical structure of BC. The BC is hydrophilic material that is expected to absorb water [10] and also BC have three-dimensional network with large amount of pores. From this study it is also concluded that even the drying methods is simple, using room temperature and not freeze drying method, the swelling ability is maintained at high capability. The high swelling ability of Ag-BC composites is important property for wound dressing that used to control wound exudates and keep moist environment on the wound [17].

### Antibacterial Activity Studies

The photographs of Ag-BC composites with different molar ratio of  $\text{NaBH}_4:\text{AgNO}_3$  are showed in Figure 6, while the Table 3 presented the inhibition zone of Ag-BC composites against four bacteria. To measure the inhibition zone, the pellicle of Ag-BC composites was cut into a circular disk of about 10 mm in diameter.



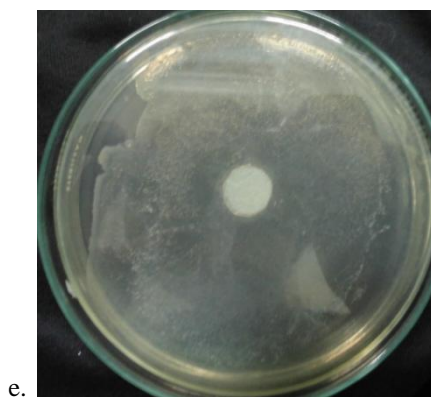


Figure 6: Photographs of antibacterial performance of Ag-BC composite against bacteria: (a) *P. aeruginosa* (b) *E. coli* (c) *S. typhi* and (d) *S. aureus*. (e) pure BC as control

The antibacterial activity of Ag-BC composites for *P. aeruginosa*, *E. coli*, *S. typhi* and *S. aureus* was measured by disc diffusion method. The disc diffusion method was adopted since the inhibition zone can be directly measured, which is one of the popular methods to establish the antibacterial activity. It was found that the room temperature-dried Ag-BC composites exhibit an inhibition zone as seen in Figure 6 and Table 3.

**Table 2:** Inhibition zone of Ag-BC composites against *E. coli*, *P. Aeruginosa*, *S. aureus* and *S. typhi*

Samples	Bacteria	Inhibition zone (mm)
A	<i>E. coli</i>	1.47±0.01
B	<i>E. coli</i>	1.28±0.01
C	<i>E. coli</i>	1.19±0.01
A	<i>P. Aeruginosa</i>	1.89±0.01
B	<i>P. Aeruginosa</i>	1.69±0.01
C	<i>P. Aeruginosa</i>	2.03±0.01
A	<i>S. aureus</i>	1.22±0.01
B	<i>S. aureus</i>	0.4±0.01
C	<i>S. aureus</i>	0.46±0.01
A	<i>S. typhi</i>	1.27±0.01
B	<i>S. typhi</i>	1±0.01
C	<i>S. typhi</i>	1.02±0.01

A: Ag-BC composites with  $\text{NaBH}_4:\text{AgNO}_3$  molar ratio of (10:1); B: (50:1) C: (100:1). No inhibition zone was observed for pure BC. The inhibition values are shown as the mean  $\pm$  SD from three independent experiments.

No inhibition zone was observed with the pure BC as control. This clearly demonstrated that the antibacterial activity is only due to Ag NPs that was modified inside BC. It was observed that the room temperature-dried Ag-BC composites were effectively inhibiting the growth of bacteria *P. aeruginosa*, followed by *E. coli*, *S. typhi* and *S. aureus*.

### Conclusion

In conclusion, Ag NPS were successfully impregnated into BC matrix to make Ag-BC nanocomposites. The highly porous BC and three dimensional networks of BC as substrate favored the diffusion of silver ion and accelerated the impregnation of ionic silver. The impregnation of silver to the BC was confirmed by morphological analysis. The room temperature-dried Ag-BC composites exhibited good antibacterial activity against *P. aeruginosa*, *E. coli*, *S. typhi* and *S. aureus*. This results show that Ag-BC composite could be potential candidate in general wound dressing and other wound healing cases.



### Conflict of interest statement

We declare that we have no conflict of interest.

### Acknowledgments

We thank Ms. Dwi Ratih and Mr. Andri Suwanto from the Research Unit for Natural Product Technology LIPI for the technical assistance. This study was financially supported by Indonesian Ministry of Research, Technology, and Higher Education (Kemenristekdikti), Indonesia through INSINAS Grant 2017 No: 04/INS-2/PPK/E/E4/2017.

### References

1. Delmer, D. P. and Amor Y. (1995). Cellulose biosynthesis. *Plant Cell*, 7: 987–1000.
2. Nishiyama, Y., Langan, P., and Chanzy, H. (2002). Crystal structure and hydrogen-bonding system in cellulose I $\beta$  from synchrotron X-ray and neutron fiber diffraction. *J. Am. Chem. Soc.*, 124: 9074–9082.
3. Ross P., Mayer, R., and Benziman M. (1991). Cellulose biosynthesis and function in bacteria. *Microbiol. Rev.*, 55: 35–58.
4. Klemm, D., Heublein, B., Fink, H. P., and Bohn. (2005). A Cellulose: fascinating biopolymer and sustainable raw material. *Angew. Chem. Int. Ed.*, 44: 3358–3393.
5. Huang, Y., Zhu, C., Yang, J., Nie, Y., Chen, C., and Sun, D. (2014). Recent advances in bacterial cellulose. *Cellulose*, 21: 1–30.
6. Wu, Z. Y., Liang, H. W., Chen, L. F., Hu, B. C., and Yu, S. H. (2016). Bacterial cellulose: a robust platform for design of three dimensional carbon-based functional nanomaterials. *Acc. Chem. Res.*, 49: 96–105.
7. Jesus, E. G., Andres, R. M., and Magno, E. T. (1971). A study on the isolation and screening of microorganism for production of diverse textured nata. *Philip. J. Sci.*, 100: 41–53.
8. Zhang, S. and Luo, J. (2011). Preparation and properties of bacterial cellulose/alginate blend bio-fibers. *J. Eng. Fiber. Fabr.*, 6: 69–72.
9. Czaja, W., Romanovicz, D., and Brown, R. M. (2004). Structural investigations of microbial cellulose produced in stationary and agitated culture. *Cellulose*, 11: 403–411.
10. Klemm, D., Schumann, D., Udhart, U., and Marsch, S. (2001). Bacterial synthesis cellulose-artificial blood, vessel for microsurgery. *Prog. Poly. Sci.*, 26: 156–1603.
11. Watanabe, K., Tabuchi, M., Morinaga, Y., and Yoshinaga, F. (1998). Structural features and properties of bacterial cellulose produced in agitated culture. *Cellulose*, 5: 187–200.
12. Czaja, W., Krystynowicz, A., Bielecki, S., and Brown Jr, R. M. (2006). Microbial cellulose – the natural power to heal wounds. *Biomaterials*, 27: 145–151.
13. Trovatti, E., Silva, N. H., Duarte I. F., Rosado, C. F., Almeida, I. F., Costa, P., Freire, C. S., Silvestre, A. J., and Neto, C. P. (2011). Bacterial cellulose membranes as supports for dermal release of lidocaine. *Biomacromolecules*, 12: 4162–4168.
14. Prashant, R. C., Ishwar, B. J., Shrikant, A.S., and Rekha, S.S. (2008). Microbial cellulose: fermentative productions and applications. *Food Technol. Biotechnology*, 47: 107–124.
15. Vandamme, E. J., Baets, S. D., Vanbaelen, V., Joris, K., and Wulf, P. D. (1998). Improved production of bacterial cellulose and its application potential. *Polym. Degrad. Stab.*, 59: 93–99.
16. Pal, S., Nisi, R., Stoppa, M., and Licciulli, A. (2017). Silver-functionalized bacterial cellulose as antibacterial membrane for wound-healing applications. *ACS Omega*, 2: 3632–3639.
17. Maneerung, T., Tokura, S., and Rujiravanit, R. (2008). Impregnation of silver nanoparticles into bacterial cellulose for antimicrobial wound dressing. *Carbohydr. Polym.*, 72: 43–51.
18. Rieger, K. A., Cho, H. J, Yeung, H.F., Fan, W., and Schiffman, J. D. (2016). Antimicrobial activity of silver ions released from zeolites immobilized on cellulose nanofiber mats. *ACS Appl. Mater. Interfaces*, 8:



3032–3040.

19. Cho, K. H.; Park, J. E., Osaka, T., and Park, S. G. (2005). The study of antimicrobial activity and preservative effects of nanosilver ingredient. *Electrochim. Acta*, 51: 956–960.
20. Percival, S. L., Bowler, P. G., and Russell, D. (2005). Bacterial resistance to silver in wound care. *J Hosp Infect*, 60: 1–7.
21. Bao, H., Yu, X., Xu, C., Li, X., Li, Z., Wei, D., and Liu Y. (2015). New toxicity mechanism of silver nanoparticles: promoting apoptosis and inhibiting proliferation. *PLoS One*, 10: No. e0122535.
22. Almeida, I. F., Pereira, T., Silva, N. H. C. S., Gomes, F. P., Silvestre, A. J. D., Freire, C. S. R., Sousa Lobo, J. M., and Costa, P. C. (2014). Bacterial cellulose membranes as drug delivery systems: An in vivo skin compatibility study. *Eur. J. Pharm. Biopharm*, 86: 332–336.
23. Zhu, C., Li, F., Zhou, X., Lin, L., and Zhang, T. (2014). Kombucha- synthesized bacterial cellulose: preparation, characterization, and biocompatibility evaluation. *J. Biomed. Mater. Res. Part A*, 102: 1548–1557.
24. Segal, L., Creely, J. J., Martin, A. E., and Conrad, C. M. (1959). An empirical method for estimating the degree of crystallinity of native cellulose using the X-ray diffractometer. *Tex. Res. J.*, 29: 786–794.
25. Cui, Q., Zheng, Y., Lin, Q., Song, W., Qiao, K., and Liu, S. (2014). Selective oxidation of bacterial cellulose by  $\text{NO}_2\text{-HNO}_3$ . *RSC Adv.*, 4: 1630–1639.
26. He, J., Kunitake, T., and Nakao, A. (2003). Facile in situ synthesis of noble metal nanoparticles in porous cellulose fibers. *Chem. Mater.*, 15: 4401–4406

